Check for updates

RESEARCH ARTICLE

Key Points:
- Low O_2 reduction rates result in low denitrification potential
- Denitrification lag times are in the order of approximately one century
- Estimation of denitrification lag times improves understanding of the self-purification potential of groundwater ecosystems

Decadal Delays in Groundwater Recovery from Nitrate Contamination Caused by Low O_2 Reduction Rates

Lisa M. Wild[1], Bernhard Mayer[2] (iD), and Florian Einsiedl[1] (iD)

[1]Chair of Hydrogeology, Faculty of Civil, Geo and Environmental Engineering, Technical University of Munich, Munich, Germany, [2]Department of Geoscience, University of Calgary, Calgary, Alberta, Canada

Abstract Nitrate (NO_3^-) is one of the main pollutants in agriculturally impacted groundwater systems. The availability and reactivity of electron donors control the prevalent redox conditions in aquifers and past nitrate contamination of groundwater can be ameliorated if denitrification occurs. Using aqueous geochemistry data and the stable isotope composition of dissolved nitrate ($\delta^{15}N$ and $\delta^{18}O$), we found that nitrate concentrations above the World Health Organization drinking water guideline were caused predominantly by manure and to a lesser extent by synthetic fertilizer applications and that denitrification was not a significant nitrate removal process in an aquifer in southern Germany underlying agricultural land with intensive hog farming. We also applied environmental isotopes (δ^2H and $\delta^{18}O$, $^3H/^3He$, and ^{14}C) linked with a lumped parameter approach to determine apparent mean transit times (MTT) of groundwater that ranged from <5 years to >100 years. Furthermore, we determined low reduction rates of dissolved oxygen (O_2) of 0.015 1/year for first-order kinetics. By extrapolating the O_2 reduction rates beyond the apparent MTT ranges of sampled groundwater, denitrification lag times (time prior to commencement of denitrification) of approximately 114 years were determined. This suggests that it will take many decades to significantly reduce nitrate concentrations in the porous aquifer via denitrification, even if future nitrate inputs were significantly reduced.

1. Introduction

Nitrate contamination in groundwater is a widespread problem in Europe, North America, Asia, and elsewhere. The European Commission (EU) drinking water limit for nitrate is 50 mg/L (0.8 mmol/L; The Council of the EU, 1998). However, the nitrate drinking water maximum allowable concentration is often exceeded in groundwater, in part due to excessive use of synthetic fertilizers and manure in agriculture. Especially, the influence of intensive livestock farming on drinking water quality has become a concern in the last decades (Hansen et al., 2011; Hooda et al., 2000). According to the status report 2012 of the European Environmental Agency, approximately 25% of all aquifers across Europe are in a poor chemical status, for which mainly nitrate contamination is responsible (Werner & O'Doherty, 2012). Furthermore, 33% of all groundwater bodies are affected by diffuse pollution from agriculture, and contrary to expectations and major efforts to reduce nitrate inputs into aquifers through changes in land use, land management, and other measures (Suchy et al., 2018), some EU countries have not met the objectives of the European Water Framework Directive to not further deteriorate and improve the chemical water quality status by 2015 (European Commision, 2015; European Community, 2000; Voulvoulis et al., 2017). A lack of timely response to such measures in the level of nitrate contamination in groundwater has puzzled stakeholders and has prompted the EU to delay its aspiration for *good qualitative status* for all EU water bodies by more than a decade, from 2015 to 2027 (European Commision, 2012). A key scientific question in this context is the residence time of nitrate in groundwater that is determined by transport processes and redox reactions that occur along groundwater flow paths.

The transport of nitrate in groundwater under oxic redox conditions can be assumed to be conservative since nitrate shows no or only little sorption effects on the aquifer matrix and does not precipitate as mineral phase (Hamdi et al., 2013; Harper, 1924; Singh & Kanehiro, 1969). In such oxic aquifers, the residence time of nitrate in groundwater may vary from less than 1 year to several decades or even centuries depending on the apparent mean transit times (MTT) of groundwater (Koh et al., 2010; Sebilo et al., 2013; Wassenaar et al., 2006). Fogg et al. (1984), for instance, estimated the vulnerability of groundwater to nitrate contamination by modeling its transport in both the vadose zone and the aquifer to produce travel time maps of the Salinas Valley, California,

that may indicate nitrate-vulnerable zones. Furthermore, apparent groundwater MTTs have been successfully determined combining environmental isotope measurements and the use of transport models (Böhlke, 2002; Einsiedl & Mayer, 2006; Maloszewski & Zuber, 1982).

An accelerated removal of dissolved nitrate from aquifers at time scales faster than the apparent MTT of groundwater can only occur through the redox processes denitrification and anammox (anaerobic ammonium oxidation). Redox reactions follow a systematic order, which is defined by the free Gibbs-Energy. An organic or inorganic electron donor, thus, favors an acceptor holding the highest free energy available. Dissolved O_2 (−501 kJ) is first consumed; subsequently, nitrate (−476 kJ), then manganese(IV) (−340 kJ), and subsequently iron(III) (−116 kJ) is reduced, followed by bacterial sulfate reduction (−102 kJ), and finally methanogenesis occurs with −93 kJ (Rivett et al., 2008). Consequently, O_2 must be first depleted before nitrate and other electron acceptors are able to react with the available electron donors such as DOC (dissolved organic carbon), FeS_2, and Fe(II) in the groundwater system. The transition from O_2 reduction to denitrification has been determined to commence at O_2 concentrations of <60 μmol/L in aquifers (Böhlke et al., 2002; Tesoriero & Puckett, 2011). Other case studies, however, indicate O_2 threshold values for the denitrification commencement of as low as 0.3 μmol/L (Calderer et al., 2010; Starr & Gillham, 1993; Vogel et al., 1981).

In laboratory studies, the availability of dissolved O_2 was found to be an important factor for the efficiency of denitrification processes and it was suggested that nitrate reduction was not most efficient under strictly anaerobic conditions (Payne, 1983; Tiedje, 1988). For instance, it was reported that the enzymes involved in the different steps of denitrification, such as nitrate (NaR), nitrite (NiR),and N_2O (N_2OR) reductase revealed different O_2 threshold concentrations (Bonin et al., 1989; Davies et al., 1989; Hochstein et al., 1984; Körner & Zumft, 1989; Robertson & Kuenen, 1984). Therefore, O_2 represents an important factor limiting the commencement of denitrification in groundwater, and the term *denitrification lag time* refers to the period required to reduce O_2 concentrations in groundwater to levels low enough so that denitrification can occur. Although some studies have focused on denitrification with the role of O_2 concentrations on nitrate turnover, the determination of O_2 reduction rates that allow the estimation of potential nitrate reduction processes has received only limited attention (Böhlke & Denver, 1995; Einsiedl et al., 2009; Katz et al., 2004; Stoewer et al., 2015; Tesoriero & Puckett, 2011; Tesoriero et al., 2000). Other factors potentially limiting denitrification include the availability of electron donors such as DOC, FeS_2, and Fe(II) (Einsiedl et al., 2007; Schwientek et al., 2008; Smith et al., 2016).

The stable isotope composition of nitrate has been successfully used to determine sources of nitrate causing a deterioration of groundwater quality in catchments with intensive anthropogenic N inputs from synthetic fertilizers, manure, waste waters, and septic systems among others (Aravena et al., 1993; Böhlke, 2002; Böhlke et al., 2002; Choi et al., 2007; Kendall & McDonnell, 1998; Mayer et al., 2002). In addition, patterns of decreasing nitrate concentrations coupled with enrichment of ^{15}N and ^{18}O in the remaining nitrate along a groundwater flow path have been shown to be an effective indicators of denitrification in aquifers (Boettcher et al., 1990; Böhlke et al., 2002; Knöller et al., 2011; Koh et al., 2010; Mariotti et al., 1988; Schwientek et al., 2008; Sebilo et al., 2006; Wassenaar, 1995). Therefore, the combination of aqueous (geo)chemical and isotopic techniques is an effective approach to determine O_2 threshold concentrations for denitrification and the extent to which nitrate reduction occurs in aquifers. If this information is combined with knowledge of apparent groundwater MTTs, it appears possible to estimate O_2 reduction rates and the time frames required to reduce O_2 in an aquifer to levels where denitrification can commence (denitrification lag time) so that nitrate removal from groundwater can be accelerated dependent on the availability of electron donors in the system. By combining information from O_2 concentration measurements, environmental isotope data, chemical parameters, and calculated apparent MTTs of groundwater, we explore whether low O_2 reduction rates represent a limiting factor that delays recovery of nitrate-contaminated porous aquifers over time scales of years or even decades.

To achieve this goal, we investigated a nitrate-contaminated aquifer in an area with intensive hog farming in southeastern Germany with the objective to determine O_2 reduction rates and to use the stable isotope composition of dissolved nitrate ($\delta^{15}N$ and $\delta^{18}O$) to evaluate nitrate sources and the extent to which denitrification has occurred in groundwater. For that, we also determined the apparent MTT of the groundwater using environmental isotopes (δ^2H and $\delta^{18}O$, $^3H/^3He$, and ^{14}C) linked with a lumped parameter modeling approach. By comparing O_2 reduction rates with apparent MTTs of groundwater, we estimated the denitrification lag time in the investigated aquifer.
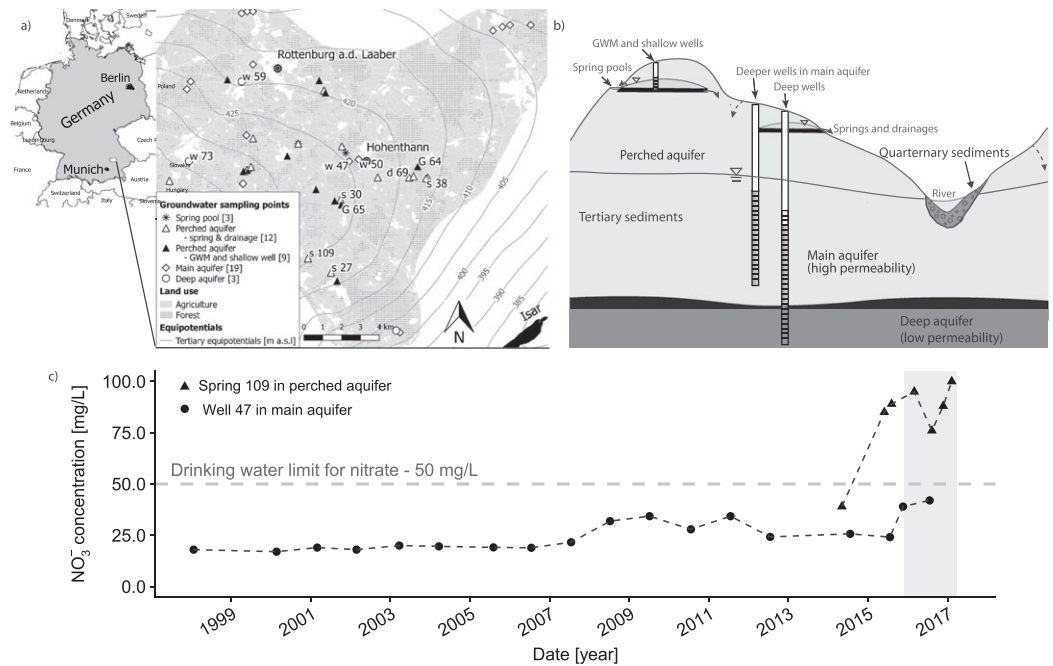
Figure 1. (a) Location of sampling sites (d = drainage, s = spring, G = GWM, w = well), (b) schematic cross-section of the hydrogeology, and (c) trend of nitrate concentrations with time for spring 109 and well 47; shaded area shows sampling period.

2. Material and Methods

2.1. Study Site, Geology and Hydrogeology

The study was conducted in a 270-km² agricultural area near Hohenthann located 90 km northeast of Munich (Bavaria, Germany) within the Bavarian Tertiary Molasse-Hills. Sixty-five percent of the area is agriculturally used with maize as the predominant crop and intensive hog farming, whereas the remaining 35% are forested and urban areas as displayed in Figure 1a. The central village Hohenthann has a population of around 4,000 inhabitants, and the hog farms in its surroundings house 65,000 pigs (Lill, 2013). According to a farmer's survey, manure and mineral fertilizer were applied in equal amounts to the fields. The area receives annual rainfall of around 800 mm (Kainzmaier et al., 2007). The mean annual air temperature is 7.5 to 8.0 °C.

Since there are no major rivers and large creeks, surface runoff of N compounds is assumed to be very limited. Hence, most of the agricultural nitrate may reach the hydrosphere mainly via groundwater recharge through sandy to silty soils at quite variable recharge rates due to the heterogeneity of the materials in the water-unsaturated zone. As the landscape is compiled of rolling hills, the depth to the saturated zone is quite variable and ranges between 0.4 and 53 mbgl with a median of 16.6 mbgl. There are hardly any wetlands and riparian zones that could facilitate denitrification or anammox during nitrate infiltration into the aquifer. Within the catchment, a hydrological divide runs east-west demarcating a boundary where groundwater flows to the northwest or southwest, toward the rivers Danube (not shown in Figure 1a) and Isar. From the hydrogeological point of view, the groundwater is hydraulically connected to the surface water and could discharge to both rivers. Consequently, the discharge of groundwater with elevated nitrate concentrations into surface water could result in a significant decrease of surface water quality. The study area is underlain by various aquifers in heterogeneous clastic sediments of the South-German Molasse basin as displayed in a schematic cross section in Figure 1b. A perched aquifer at depths above 45 mbgl is formed by locally occurring clay layers with coarser sand and gravel above with groundwater being partly discharged to springs. The main aquifer from 45- to 150-m depth is composed of the Younger Upper Freshwater Molasse (UFMy), the Northern Gravel Series, and the Fluviatile Freshwater Layers of the upper freshwater molasse (UFM). The facies is described as sandy, gravelly to silty, with K_f values of 10^{-6} to 10^{-4} m/s (Kainzmaier et al., 2007). A deep aquifer in 150- to 200-m depth in the limnic freshwater layers belongs to a sequence of fine clastic sediments and is located underneath the UFM and the main aquifer. The facies includes purple-colored sandy clays and marl together with light brown micaceous fine- to medium-grained sand. The limnic freshwater layers belong to the Upper

Brackish Molasse (late Ottnangian/early Kapatian) and the hydraulic conductivities are lower with K_f values between 8×10^{-7} and 5×10^{-5} m/s (Doppler et al., 2005; Kainzmaier et al., 2007).

The groundwater recharge for the perched aquifer ranges between 54 and 89 mm/a, whereas the recharge for the main aquifer is much less with around 16 mm/a (Kainzmaier et al., 2007). For the deep aquifer, no recharge rates have been determined.

Nitrate concentrations are generally high in groundwater of the study area and displayed often increasing trends throughout the last two decades. For instance, nitrate concentrations in groundwater from well 47 completed in the main aquifer increased from 18 mg/L (0.29 mmol/L) in 1998 to 44 mg/L (0.71 mmol/L) in 2016, while a spring (#109) draining groundwater from the perched aquifer had nitrate concentrations increasing from 39 mg/L (0.63 mmol/L) in 2014 to 100 mg/L (1.61 mmol/L) in 2017 as displayed in Figure 1c.

2.2. Sampling

Sampling was conducted within a project campaign of the Bavarian Environmental Agency between December 2015 and March 2017, with the main sampling of deep wells conducted in the summer of 2016. During the sampling campaign three spring pools, which are springs draining into small surface water ponds ($n = 3$), 12 springs and tile drainages ($n = 12$), and nine ($n = 9$) shallow groundwater monitoring (GWM) and domestic wells, all yielding groundwater from the perched aquifer were sampled. In addition, 22 deep groundwater wells ($n = 22$) were sampled once, of which 19 wells are screened in the main aquifer ($n = 19$) and three in the deep aquifer ($n = 3$). One electrically cooled precipitation collector was sampled every month. All sampling points are displayed in Figure 1a.

The field parameters electrochemical conductivity (EC), pH, redox potential (E_h), temperature (T), and the dissolved O_2 concentration were determined in the field for groundwater from wells after either exchanging at least $1.5 \times$ the volume of the standing water in the wells or after physicochemical parameters had stabilized while measuring them continuously using a flow cell. For springs and drainages, these parameters were measured directly in the outflow or in a beaker. Samples for major and minor anions (filtered, unacidified) and cations (filtered and acidified) were obtained from all sampling points and analyzed in the laboratory for concentrations. To determine the sources of dissolved nitrate and to assess whether denitrification had occurred, samples for nitrogen (N) and oxygen (O) isotope analyses were obtained from all deep groundwater wells and the spring-fed pond once, while such samples were collected every 3 months for seepage waters of the agriculturally used fields and the forested areas from 12 drainages and springs and from the nine GWM and shallow domestic wells. To characterize the apparent MTT of groundwater, samples for the determination of the isotopic composition of water (δ^2H and δ^{18}O) were collected monthly from four selected springs and the four GWM completed in the perched aquifer and the precipitation collector. Every 3 months samples were obtained from the shallow domestic wells in the perched aquifer and once in summer 2016 from 19 deeper wells (> 45 mbgl) that were screened in the main aquifer. From these wells, samples were also obtained for the analysis of ^{3}H / ^{3}He. Three deep wells completed and screened in the deep aquifer (134.5 to 185 mbgl) were sampled for the same parameters as all other wells plus an additional sample for ^{14}C was obtained.

2.3. Standard Parameters and Major Ions

The physicochemical parameters EC, pH, redox potential (E_h), temperature, and the dissolved O_2 concentration were measured in the field using a flow cell for groundwater from all wells.

Major ions in the water (Na^+, NH_4^+, K^+, Mg^{2+}, Ca^{2+}, F^-, Cl^-, NO_2^-, Br^-, NO_3^-, PO_4^{3-}, and SO_4^{2-}) were analyzed with a Sykam ion chromatograph (SYKAM Chromatographie Vertriebs GmbH, Fürstenfeldbruck, Germany). Anion concentrations were determined with a Dionex IonPac AS22 analytical column (4×250 mm) and cations with a Dionex IonPac CS 12A analytical column (4×250 mm) (Thermo Fischer Scientific, MA, USA).

DOC concentrations were determined with a Analytik Jena TOC analyzer Multi N/C® 3100/2100 (Analytik Jena AG, Jena, Germany) with an analytical error of approximately $\pm 15\%$ at a DOC concentration of ≈ 0.08 mM. The detection limit of DOC was 16.7 μmol/L; however, 11.8 μmol/L is the calculated lower concentration c_L, where all measured data below the detection limit (d) of 16.7 μmol/L is displayed as $c_L = d/\sqrt{2} = 11.78$ μmol/L.

2.4. The Isotopic Composition of Water (δ^2H and δ^{18}O)

To determine the isotopic composition of water (δ^2H and δ^{18}O), the samples were filtered with a 0.22-μm filter and filled into a 2-mL-Vial in the field. Hydrogen and oxygen isotope ratios of water were measured with a *Triple-Liquid Water Isotope Analyzer*, which is a infrared spectrometer for isotopic ratios from the company

Los Gatos Research. The analytical precision is ± 0.15‰ for $\delta^{18}O$ and ± 1‰ for δ^2H. Hydrogen and oxygen isotope ratios are expressed in the internationally accepted δ notation shown in equation (1) with respect to the standard Vienna-Standard Mean Ocean Water.

$$\delta[‰] = \frac{R_{Sample} - R_{Standard}}{R_{Standard}} \tag{1}$$

where R stands for $^2H/^1H$, $^{15}N/^{14}N$ or $^{18}O/^{16}O$ of samples and references, respectively

2.5. Nitrate isotopes ($\delta^{15}N$ and $\delta^{18}O$)

For N and O isotope ratio analysis of nitrate, NO_3^- was extracted from groundwater samples using the methodology of Silva et al. (2000). From the formed anhydrous $AgNO_3$, 300 μg was transferred into a tin cup for nitrogen isotope analysis and 1000 μg into a high-purity silver cup for analysis of the O isotope ratios of NO_3^-. Samples were thermally decomposed in an elemental analyzer and the resulting N_2 was analyzed by isotope ratio mass spectrometry (IRMS) in a continuous flow mode. To determine O isotope ratios of NO_3^-, CO was generated through pyrolysis using a High Temperature Conversion Elemental Analyzer (TC/EA) reactor (1350 °C) coupled to a delta plus XL IRMS in continuous flow mode (Einsiedl & Mayer, 2006). Nitrogen and oxygen isotope ratios of nitrate are expressed in the standard δ (delta) notation in per mill (‰) as calculated in equation (1) with respect to the international standards nitrogen (N_2) in atmospheric air (AIR) for $\delta^{15}N$ and Vienna-Standard Mean Ocean Water for $\delta^{18}O$. The uncertainty of the method is ± 0.5‰ for both $\delta^{15}N$ and $\delta^{18}O$.

2.6. Sulfur Isotope Ratios ($\delta^{34}S$) of Sulfate

To analyze S isotope ratios in SO_4^{2-}, sample volumes of 1 L were acidified to pH ≤ 3 and $BaCl_2$ (10%) was added to precipitate $BaSO_4$, which was then filtered and dried. Isotope analysis was performed by IRMS after complete conversion of $BaSO_4$ to SO_2 via high temperature combustion (1000°) with V_2O_5 in an elemental analyzer.

2.7. Tritium and Helium ($^3H/^3He$)

Samples for tritium analyses were collected in duplicates in 1 L plastic bottles. Samples for helium isotopes and neon (Ne) analyses were collected in duplicates in copper tubes following the sampling protocol of the Institute of Environmental Physics, Bremen University (http://www.noblegas.uni-bremen.de/documents/sampling_hints.pdf). He and Ne were extracted from the water and separated from other gases using a cryo system at 25 K and 14 K. ^4He, ^{20}Ne, and ^{22}Ne analyses were conducted with a quadrupole mass spectrometer (Balzer QMG112A), helium isotopes were measured with a high-resolution sector field mass spectrometer (MAP 215-50), and tritium was analyzed with the ^3He-ingrowth method (Massmann et al., 2007; Sültenfuß et al., 2009). Ne was analyzed to identify potential atmospheric contamination excess air in ^3He samples. If there is excess air in the sample, which may be determined by Δ^4He being smaller than ΔNe, fractionation might have taken place and the sample was discarded. The measurement error for ^3H is less than 0.01 TU and the error for ^3He is determined by the uncertainty of air excess and the infiltration temperature and is estimated to 2% at an equilibrium concentration (Sültenfuß, 1998; Sültenfuß & Massmann, 2004).

2.8. Carbon-14 (^{14}C)

For each of the three deep wells, 2×1 L of groundwater was collected in plastic bottles for carbon-14 analysis (^{14}C) on dissolved inorganic carbon. The samples were analyzed in an Acceleration Mass Spectrometer at the GADAM Centre in the Silesian University of Technology, Gliwice, Poland, following the protocol of Piotrowska (2013).

2.9. Modeling of Mean Transit Times

Apparent MTT of groundwater were modeled with a lumped parameter model that is characterized by the transit time distribution function of tracer particles transported between the input (recharge area) and the output (well or a spring). For the interpretation of environmental isotope data (δ^2H and $\delta^{18}O$, ^3H, ^3He, and ^{14}C) we used the dispersion model as shown in equation (2) (Einsiedl et al., 2009; Kreft & Zuber, 1978; Maloszewski & Zuber, 1982, 1996, 1985) and as modeling software the Excel workbook TraceLPM (Jurgens et al., 2012; Visser et al., 2013).

$$g(\tau) = \frac{1}{\sqrt{4\pi P_D^* \tau/T^*}} \times \frac{1}{\tau} \times \exp[-\frac{(1 - \tau/T^*)^2}{4P_D^* \tau/T^*}] \tag{2}$$

Where τ is the integration of the transit time distribution, T^* the transit time of the tracer and in favorable conditions equal to the mean age of water (T) and P_D^* the apparent dispersion parameter (inverse of the Peclet number)

If theoretical output concentrations could not be fitted to the isotope concentrations measured in groundwater with a simple dispersion model, it was assumed that groundwater mixing between old ^{3}H-free (old fraction) and young groundwater due to well screens across multiple aquifer units in a well had occurred. For finding a model fit for groundwater that is characterized by an old tritium-free and young ^{3}H containing water component a Binary Mixing Model (BMM) was used. Here the BMM is defined by two dispersion models for the first and second water components (Jurgens et al., 2012). To estimate the apparent groundwater ages of data points that were modeled with a Binary Mixing Model, the second water component was assumed ^{3}H-free and therefore 500 years was set as the MTT and a P_D^* of 0.1 was chosen. However, if there was no good model fit or no realistic MTT and P_D^* for the first component found, the P_D^* of the second water component was changed slightly to obtain less error.

In the dispersion model, the two parameters P_D^* and the MTT are used as fitting parameters and can be found by solving the convolution integral along with the used lumped parameter approach (Maloszewski & Zuber, 1982). The proximity of the investigated catchment area to Munich (90 km), allowed using ^{3}H data that were taken from a precipitation station in Munich, Neuherberg (Germany). However, the data set was extended by extrapolation with International Atomic Energy Agency (IAEA) data from Vienna, Austria, as for the years January 2007 toJuly 2009 when no data from Munich were available. Precipitation data were added from the Germany's National Meteorological Service data base for the weather station Munich, Neuherberg. To obtain a more realistic input signal, the raw input data were adjusted by equation (3) using the yearly weighted precipitation means of Neuherberg, Munich, Germany, and an alpha factor of 0.44 that was calculated by using equation (4), including the precipitation and δ^{18}O data from 1998 to 2002 from Munich, Neuherberg (Grabczak et al., 1984).

$$c = \frac{\sum_i \alpha_i P_i c_i}{\sum_i \alpha_i P_i} \tag{3}$$

$$\alpha = \frac{|(\delta P_W - \delta G)\sum_i (P_i)_W|}{|(\delta G - \delta P_S)\sum_i (P_i)_S|} \tag{4}$$

where δG stands for the mean δ^{18}O value of the local groundwater originating from recent precipitation; δP_W and δP_S are the long-term weighted mean δ^{18}O values for the winter and summer precipitation, respectively.

Theoretical ^{3}H output concentrations that were found with the dispersion model were fitted to the tracer time series of ^{3}H in groundwater. If no ^{3}H timeline was available, a tracer-tracer model calculated the apparent MTT for given measured ^{3}H, ^{3}He concentrations the initial tritium concentration ^{3}H$_0$ and ^{14}C. In comparison to the tracer time series application of the Tracer-LPM, the tracer-tracer model evaluates multiple tracer output concentrations with modeled concentrations against each other at a single sampling event (Jurgens et al., 2012). Further, the theoretical output concentration of ^{3}He was also fitted to the measured ^{3}He concentrations in groundwater that were collected for the wells in 2016. Model fitting for time series graphs were carried out using a trial-and-error process for ^{3}H and ^{3}He. For the tracer-tracer model an automated modeling process was conducted by the program and the goodness of fit was quantitatively described by the model efficiency in percent error.

3. Results

As the physicochemical parameters, the concentrations of major ions and the compositions of stable isotopes of nitrate ($\delta^{15}N$ and δ^{18}O) only varied to a negligible extent during the sampling campaigns, we present only the results of a single sampling event.
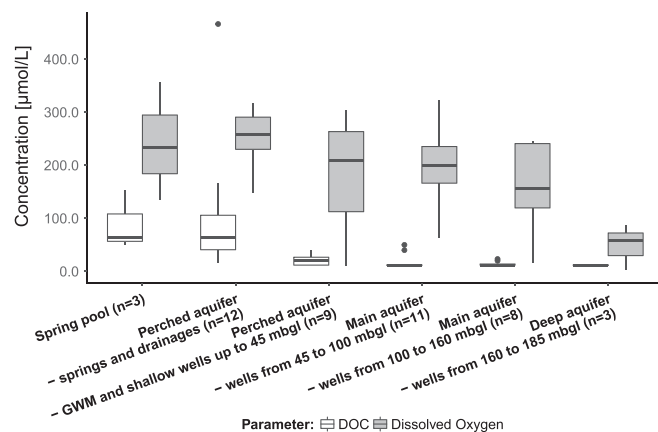
3.1. Field Parameters and Distribution of Major Ions

Groundwater in the study area is of Ca^{2+}-HCO$_3^-$ type as revealed in a Piper plot, shown in Figures S1 in the SI and there is no evidence of cation exchange between Ca^{2+} and Na$^+$. The median, maximum, and minimum values of major ions and physicochemical parameters for the three aquifers are summarized in Table 1. Nitrate concentrations varied between a minimum of 0.003 mmol/L (well 73, deep aquifer) and a maximum of 1.37 mmol/L (spring 109, perched aquifer). Almost 50% of the drainages, springs, GWM, and shallow wells

Table 1
Median, Minimum, and Maximum Values of the Physico-Chemical Parameters in the Different Aquifers

Parameter	Perched aquifer ($n = 23$)			Main aquifer ($n = 19$)			Deep aquifer ($n = 3$)		
	Median	Min	Max	Median	Min	Max	Median	Min	Max
O_2 (µmol/L)	249.1	11.0	306.9	198.8	16.6	322.8	57.5	1.9	87.2
O_2 (%)	72.9	3.4	93.7	60.2	5.1	96.5	18.4	0.6	32.2
DOC (µmol/L)	33.3	11.8	466.3	11.8	11.8	50.0	11.8	11.8	11.8
E_h (mV)	129.0	69.4	292.9	198.6	14.3	295.5	162.7	−84.4	182.0
pH (-)	7.2	6.1	8.0	7.4	7.1	7.4	7.3	7.1	7.3
EC (µS/cm) 25 °C	675.0	313.0	969.0	590.0	546.0	814.0	582.0	504.0	593.0
Temp. (°C)	10.8	7.3	11.8	10.9	10.0	17.2	13.0	12.9	16.8
HCO_3^- (mmol/L)	4.68	1.13	7.45	5.36	2.86	6.66	6.00	5.70	6.34
SO_4^{2-} (mmol/L)	0.29	0.18	0.57	0.19	0.04	0.42	0.11	0.10	0.19
Cl^- (mmol/L)	0.59	0.16	1.33	0.42	0.11	1.13	0.14	0.03	0.14
F^- (mmol/L)	0.01	0.00	0.02	0.01	0.00	0.01	0.01	0.01	0.01
NO_3^- (mmol/L)	0.76	0.11	1.31	0.33	0.08	0.90	0.10	0.00	0.11
NH_4^+ (mmol/L)	0.001	0.001	0.054	0.001	0.001	0.001	0.003	0.001	0.004
Ca^{2+} (mmol/L)	2.10	0.76	2.87	1.97	1.60	2.77	1.86	1.84	1.90
Mg^{2+} (mmol/L)	1.17	0.39	1.65	1.22	1.07	1.50	1.36	1.28	1.40
Na^+ (mmol/L)	0.25	0.13	0.45	0.16	0.13	0.38	0.23	0.17	0.24
K^+ (mmol/L)	0.02	0.01	0.16	0.02	0.01	0.04	0.03	0.02	0.03
Fe_{total} (mmol/L)	0.0	0.0	0.015	0.0	0.0	0.001	0.005	0.0	0.01

in the perched aquifer show nitrate concentrations above the nitrate drinking water maximum allowable concentration of 0.8 mmol/L and about 40% of the deeper wells in the main aquifer are above 0.4 mmol/L.

As shown in Figure 2, O_2 concentrations were highest in the perched aquifer with a median of 249.1 µmol/L and decreased slightly in the main aquifer with a median of 198.8 µmol/L and were lowest in the deep aquifer with a median of 57.5 µmol/L. DOC concentrations decreased rapidly from the spring pools and the springs and drainages in the perched aquifer with a median of 33.3 µmol/L to a median of 11.8 µmol/L in the main aquifer and the deep aquifer. Redox potentials ranged between a minimum of −84.4 mV (deep aquifer) to a maximum of +295 mV (main aquifer). Median E_h values ranged from +129 mV in the perched aquifer to +198.6 mV in the main aquifer and +162.7 mV in the deep aquifer indicating a lack of reducing conditions in the three aquifers with the exception of groundwater around well 59 in the deep aquifer (−84.4 mV). The pH values in groundwater were near neutral in all measured sampling points ranging from a pH of 6.1 to 8.0 (minimum and maximum measured in the perched aquifer).

3.2. Stable Isotope Composition of Water ($\delta^2 H$ and $\delta^{18} O$)

The oxygen and hydrogen isotope ratios of groundwater (Figure S2 in the SI) varied between −10.2‰ and −9.1‰ for $\delta^{18} O_{water}$ and −72.2‰ to −63.4‰ for $\delta^2 H$ in the perched aquifer. In the main aquifer they varied between −10.2‰ and −9.6‰ for $\delta^{18} O_{water}$ and −73.9‰ to −69.2‰ for $\delta^2 H$. In the deep aquifer, $\delta^{18} O_{water}$ and $\delta^2 H$ varied only within analytical uncertainty, ranging from −10.2‰ to −9.9‰ and from −73.6‰ to −71.4‰, respectively.

For monthly measurements of $\delta^{18} O_{water}$ and $\delta^2 H$ in the GWM and springs in the perched aquifer a larger range from −10.5‰ to −6.9‰ and −71.7‰ to −59.0‰, respectively, was observed. The amplitude between minimum and maximum $\delta^2 H$ values showed a range from 1.0‰ to 3.9‰ for groundwater from GWM and shallow domestic wells in the perched aquifer and from 0.9‰ to 11.8‰ for springs in the perched aquifer with drainage 69 showing by far the largest variance of 11.8‰ over a period of 1 year. The

Figure 2. Boxplot of dissolved O_2 and DOC concentrations (µmol/L) in different depths of the aquifer.

Table 2
Median, Minimum, and Maximum of $\delta^{15}N_{nitrate}$ and $\delta^{18}O_{nitrate}$ for the Different Aquifers

	Spring pools			Perched aquifer			Main aquifer		
	Median	Min	Max	Median	Min	Max	Median	Min	Max
$\delta^{15}N$ (‰)	12.4	11.1	13.6	8.5	-0.6	19.7	6.8	4.2	11.2
$\delta^{18}O$ (‰)	4.5	3.5	5.6	2.3	1.08	7.5	1.9	-0.5	4.0

	Deep aquifer			Overall		
	Median	Min	Max	Median	Min	Max
$\delta^{15}N$ (‰)	2.1	−5.0	6.4	7.7	-5.0	19.7
$\delta^{18}O$ (‰)	2.8	1.6	3.9	2.3	-0.5	7.5

collected rainfall from the precipitation sampling point in the study area showed unweighted $\delta^{18}O$ values from −15.2‰ to −5.1‰ and δ^2H values from −116.4‰ to −36.4‰ in the timespan of 1.5 years. The amplitude of the unweighted $\delta^{18}O$ lies therefore at 10.1‰ and for δ^2H at 80.0‰.

3.3. Stable Isotope Composition of Nitrate ($\delta^{15}N$ and $\delta^{18}O$)

Median, maximum, and minimum $\delta^{15}N_{nitrate}$ and $\delta^{18}O_{nitrate}$ values are displayed in Table 2. The most ^{15}N- and ^{18}O-enriched nitrate isotope compositions were observed for groundwater from two shallow GWM wells in the perched aquifer, showing $\delta^{15}N_{nitrate}$ values of 13.1‰ ($\delta^{18}O_{nitrate}$ = 5.2‰) for GWM 65 and 19.7‰ ($\delta^{18}O_{nitrate}$ = 7.5‰) for GWM 64 and a spring pool with 13.6‰ ($\delta^{18}O_{nitrate}$ = 3.5‰) as shown in Figure 3.

3.4. Sulfur Isotope Composition of Sulfate ($\delta^{34}S$)

Groundwater obtained from six wells/GWMs and one spring was analyzed for $\delta^{34}S$ in sulfate and values between −8.2‰ and 5.4‰ were observed. The measured $\delta^{34}S$ were plotted against $\delta^{15}N_{nitrate}$ in Figure 4 to identify chemo-lithotrophic denitrification by pyrite oxidation.

3.5. Calculation of Apparent Mean Transit Times

Apparent MTT for groundwater from wells screened in the perched aquifer varied between 5 and 20 years based on results from the dispersion model. P_D^* values ranged from 0.08 to 0.45. Groundwater MTT in the main aquifer obtained with a dispersion model ranged between 14 and 122 years, while P_D^* varied from 0.01 to 0.28. For wells completed in the main aquifer with several screen horizons, the apparent MTT of the first groundwater component were between 14 and 36 years and P_D^* values ranged from 0.01 to 0.42, assuming a second component of ^3H-free groundwater. Apparent MTTs for groundwater from wells in the deep aquifer were determined with a dispersion parameter and using the ^3H and ^{14}C concentrations. The dilution factor q describes the fractional reduction of $a_0^{14}C$ to determine a corrected $a^{14}C_{corr}$ input signal with less than 100 pMC. The q values can range from 1 (no dilution, open system) to 0.75 (minor dilution from closed system exchange) to 0.5 (closed system carbonate weathering and exchange) to less than 0.5 (extensive carbonate exchange, possible bacterial sulfate reduction; Clark, 2015). As a result, ^{14}C modeling revealed apparent MTTs from 965 to 6002 years for groundwater from wells in the deep aquifer depending on the q values ranging from 0.85 to 0.65.

3.6. Calculation of O_2 Reduction Rates

Figure 5 displays the apparent MTT against the O_2 concentrations of the groundwater samples showing a decrease of dissolved O_2 concentrations with increasing apparent MTT, although O_2 concentration did not reach values below 6.3 μmol/L. As groundwater from wells modeled with a BMM (gray triangles) did not fit a linear regression line, they were separated from those modeled with a dispersion model (black dots) and excluded from the calculation of O_2 reduction rates. A zeroth-order rate constant k_0 was determined by fitting a linear regression line to a plot of O_2 concentration against the apparent groundwater MTT calculated by the dispersion model (Appelo & Postma, 2005; Bekins et al., 1998; Böhlke et al., 2002; Tesoriero & Puckett, 2011). The linear regression line of the dispersion model MTTs showed a good coefficient of determination with
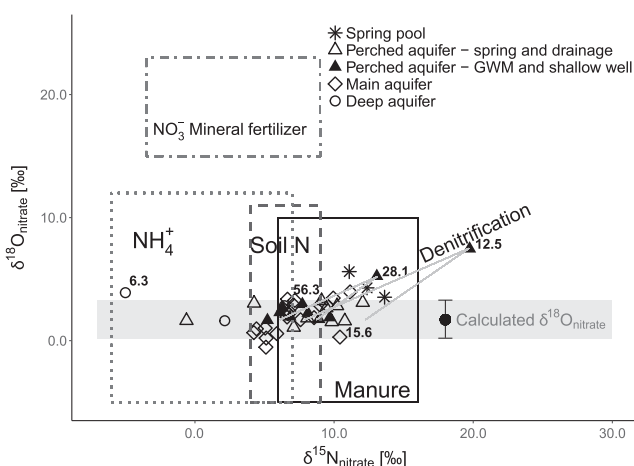
Figure 3. Plot of $\delta^{15}N_{nitrate}$ against $\delta^{18}O_{nitrate}$ to characterize nitrate sources and potential denitrification after Kendall and McDonnell (1998); O_2 concentrations (μmol/L) of less than 60 μmol/L are displayed next to data points.
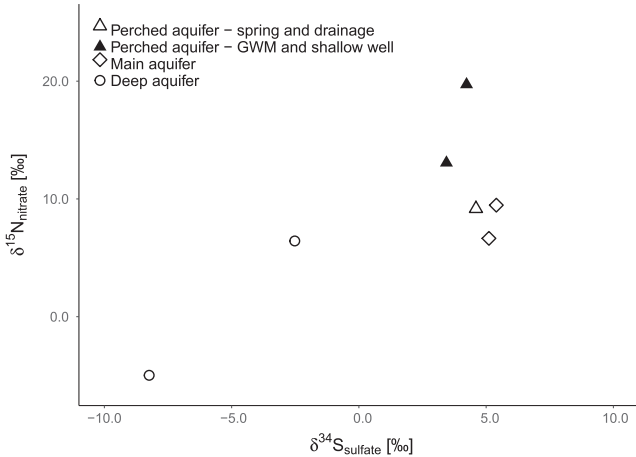
Figure 4. Plot of $\delta^{34}S_{sulfate}$ against $\delta^{15}N_{nitrate}$ to identify chemo-lithotrophic denitrification.

$R^2 = 0.77$ and a negative slope of 2.2 suggesting an O_2 reduction rate of 2.2 μmol/(L·year). A first-order rate constant k_1 was determined by fitting a linear regression line to a plot of ln(c) versus the apparent groundwater MTT (Tesoriero & Puckett, 2011). The O_2 reduction rate, determined by the first order, was 0.015 1/year with $R^2 = 0.84$.

4. Discussion

### 4.1. Aqueous Chemistry and Stable Isotopes of Water

The distribution of physicochemical parameters and major ions were typical for groundwater in the UFM (Kainzmaier et al., 2007). Kainzmaier et al. (2007) found electrical conductivities in the range of 145 to 1,070 μS/cm in the perched aquifer and 271 to 822 μS/cm in the main aquifer, while in this study EC values of up to 969 μS/cm were measured in the perched aquifer, which may be explained by the high anthropogenic contamination of the groundwater system. Moreover, nitrate concentrations are elevated in the majority of the samples of the perched aquifer and the main aquifer. In the perched aquifer, nitrate concentrations often exceed the drinking water limit of 0.8 mmol/L (The Council of the EU, 1998), and even the median nitrate concentration of 0.76 mmol/L for the perched aquifer is close to the drinking water limit of 0.8 mmol/L.

A plot of δ^2H against $\delta^{18}O$, displayed in Figure S2 in the SI indicates that all sampled groundwater has a meteoric origin and that evaporation during recharge had little influence on the isotopic composition of the sampled groundwater. The measured groundwater isotope data fit well to the Local Meteoric Water Line with δ^2H (‰) $= 7.9\ \delta^{18}O + 7.9$ of Neuherberg, Munich, Germany (Stumpp et al., 2014).

4.2. Constraints on Apparent Mean Transit Times

Since the unweighted δ^2H values of precipitation samples that were collected in the study area vary up to 80‰ within the year, seasonal variations of groundwater with short apparent MTTs of up to 4 to 5 years should be detectable (Stichler & Herrmann, 1983). Based on the variation of δ^2H values of 11.8‰ ($n = 5$) and an assumed P_D^* of 0.1, it can be concluded that groundwater of drainage 69 has a relatively short apparent MTT from a few weeks to less than 1 year. Variations in δ^2H values of more than 3‰ were also detected in groundwater from the perched aquifer in spring 30 with a δ^2H amplitude of 3.5‰ ($n = 13$), and in spring 38 with 6.5‰ ($n = 2$) indicating apparent MTTs of less than 4 years. Considering the measurement error of 1‰ for δ^2H, eight out of nine GWM/domestic wells and 9 out of 12 springs/drainages in the perched aquifer did not show a larger amplitude than 3‰, whereof only six of the springs and drainages and five of GWM/domestic wells were sampled regularly for δ^2H with at least 10 data points. These relatively low amplitudes and no seasonal variation in most of the springs, GWM, and shallow domestic wells suggest an apparent MTT of more than 4 to 5 years (Maloszewski et al., 1983, 2002; Stichler & Herrmann, 1983). The stable isotope compositions
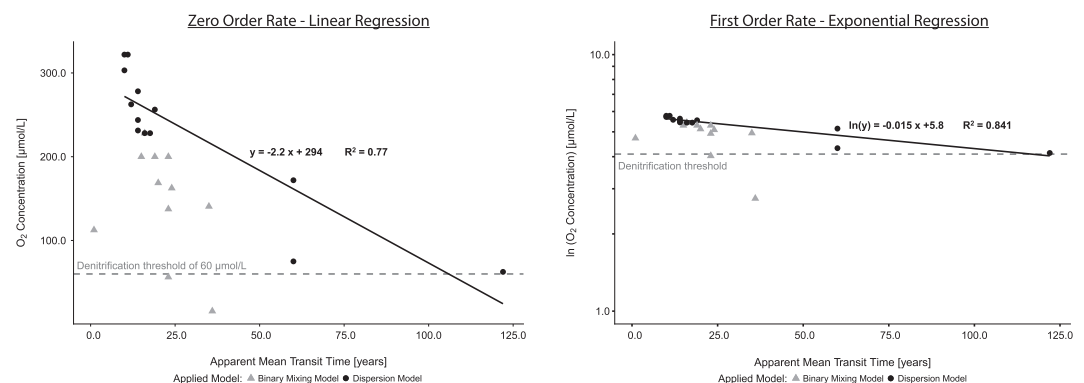
Figure 5. O_2 concentrations against the apparent MTT of groundwater modeled with a dispersion model (black dots) and a BMM (gray triangles). (a) Determination of zeroth-order rate constant k_0 by fitting a linear regression line to O_2 concentrations (C) versus apparent MTT (dispersion model). (b) Determination of first-order-rate constant k_1 by fitting a linear regression line to ln (C) versus apparent MTT (dispersion model).

of water suggest that the groundwater in the majority of springs, GWM, and shallow domestic wells in the perched aquifer have an apparent MTT of more than 4 years.

MTT modeling results using the $^3H/^3He$ method and ^{14}C as a groundwater dating tool showed that the groundwater obtained from GWM and shallow wells, screened in the perched aquifer, is relatively young ranging from 5 to 20 years, whereas a wide range of MTTs between 14 and 122 years were calculated for groundwater from the main aquifer. The large range of MTTs may be explained by the strong heterogeneity of the porous aquifer system and the varying depths of screens in the wells. In Figure 5, we display only the MTT modeling results with reasonable error percentages and P_D^* values between 0.01 and 0.3.

The plot of apparent MTTs versus O_2 concentrations (Figure 5) shows that MTTs obtained using a dispersion model can be well described with a linear regression, while apparent MTTs modeled with a BMM do not conform with the O_2 reduction of data points modeled with a simple dispersion model. Figure 5 also shows that all data points modeled with a BMM composed of two water components (gray triangles) lie below the regression line of the ones that were modeled with a dispersion model using one water component. This suggests that the groundwater in wells modeled with the BMM may be affected by mixing of at least two water components and the O_2 concentrations may be decreased only due to the influence of old, O_2-reduced water and not by O_2 reduction processes along the flow path.

4.3. Limits of Oxygen Reduction Rates

Figure 2 displays the O_2 and DOC concentrations in different depths of the aquifer. The O_2 concentrations decrease only slightly from the springs and drainages connected to the perched aquifer (median = 258.1 μmol/L) to GWM and shallow wells up to 45 mbgl of the perched aquifer (median = 210.0 μmol/L), whereas the median DOC concentration decreases from 63.3 μmol/L to 20 μmol/L, respectively. Although there are considerable stochiometric variations (Taylor & Townsend, 2010), we assumed that 1 μmol/L DOC can reduce 1 μmol/L O_2. We found that only one third of the O_2 reduction appears to be caused by DOC oxidation. This indicates that the availability of easy degradable DOC may be the limiting factor for the lack of O_2 reduction as there is either too little DOC or it is not readily available for microorganisms (Aravena & Wassenaar, 1993; Clark & Fritz, 1997; Einsiedl et al., 2007). However, there is a lack of information concerning the total organic carbon (TOC) content of the aquifer material. Within the scope of this project there was no core material available to determine the quantity and quality of TOC and its effect on O_2 reduction rates, but we suggest to further assess this in the future. Fe(II) as another electron donor may be excluded due to very low concentrations of total iron in all groundwater samples. It appears that the lack of electron donors in the aquifer may represent the limiting parameter for significant O_2 reduction and low O_2 reduction rates. Therefore, high O_2 concentrations in the groundwater may be the reason for high NO_3^- concentrations due to a lack of denitrification.

4.4. Sources of Nitrate in Groundwater

To characterize sources of nitrate and reveal potential denitrification in the groundwater system, the $\delta^{15}N$ and $\delta^{18}O$ values of dissolved nitrate from each groundwater sampling point were determined and are plotted in Figure 3.

Literature sources reveal that nitrate derived from manure has typically $\delta^{15}N_{nitrate}$ values in the range of +7 to +16‰ and $\delta^{18}O$ values of $\leq$ +5‰ (Kendall & McDonnell, 1998). This is consistent with the isotopic compositions of nitrate in the majority of the groundwater samples from the spring pools (median $\delta^{15}N$ value of 12.4‰), the perched aquifer (median $\delta^{15}N$ value of 8.5‰) and to some extent the main aquifer with a median $\delta^{15}N$ value of 6.8‰, and $\delta^{18}O$ values of nitrate <5‰ (Table 2 and Figure 3). The elevated $\delta^{15}N$ values along with high nitrate concentrations as shown in Figure 7 suggest that, especially in younger groundwater, nitrate is derived from manure (Kendall & McDonnell, 1998). During the microbial nitrification of manure-derived ammonium to nitrate, two thirds of the O_2 atoms in the newly formed nitrate are derived from water and one third from dissolved atmospheric O_2 (Amberger & Schmidt, 1987; Böhlke et al., 1997; Durka et al., 1994; Hollocher, 1984; Kendall & McDonnell, 1998; Wassenaar, 1995). The theoretically expected $\delta^{18}O_{nitrate}$ derived from nitrification can therefore be calculated to an approximate value of 1.7‰ using a $\delta^{18}O_{water}$ value of −9.2‰ and a $\delta^{18}O_{O_2}$ value of 23.5 ± 0.3‰ (Kroopnick & Craig, 1972). Voerkelius (1990) found in laboratory studies similar $\delta^{18}O$ values for nitrate that was formed by nitrification between −2 and +2‰ using $\delta^{18}O$ values for water of −10‰ that were very close to those in our study ($\delta^{18}O_{water}$ = −9.2‰).

However, recent studies have shown that the O exchange between water-oxygen, molecular O_2, and NO_2^-, as well as oxygen isotope fractionation can have a significant impact on the $\delta^{18}O_{nitrate}$ (Buchwald et al., 2012;

Casciotti et al., 2010; Fang et al., 2012; Snider et al., 2010). Therefore, $\delta^{18}O$ values of nitrate from microbial nitrification can vary widely depending on soil types, pH, and C content (Amberger & Schmidt, 1987; Einsiedl & Mayer, 2006; Mayer et al., 2001; Voerkelius, 1990). Consequently, we assigned an uncertainty of $\pm1.5‰$ to the calculated $\delta^{18}O_{nitrate}$ value of 1.7‰ that assumed no O exchange reactions and no oxygen isotope fractionation for nitrate derived from nitrification (see gray-shaded area in Figure 3). The majority of groundwater nitrate samples, except the samples from two GWMs, three spring pools, and one well in the main aquifer (well 50), fall into this predicted range of $\delta^{18}O_{nitrate}$ for nitrification processes.

In several wells, predominantly completed in the main aquifer, nitrate was observed with $\delta^{15}N_{nitrate}$ values ranging from +4 to +7‰ and $\delta^{18}O$ values of <5‰ (Figure 3). These isotope compositions are consistent with nitrate being derived from nitrification of soil N ($\delta^{15}N$ from +4 to +7‰) or possibly nitrate originating from synthetic fertilizers (typically around $0 \pm 3‰$) (Einsiedl & Mayer, 2006; Kendall & McDonnell, 1998).

Nitrate observed in groundwater from the deep aquifer with the highest MTTs had the lowest median $\delta^{15}N_{nitrate}$ value with 2.1‰ (Table 2) and $\delta^{18}O$ values <5‰ (Table 2 and Figure 3). This is consistent with nitrate being derived either from synthetic fertilizers or from nitrification processes in agricultural or forest soils throughout the catchment area (Einsiedl & Mayer, 2006). Nitrate from precipitation that undergoes immobilization with subsequent ammonification and nitrification in forest soils results in $\delta^{15}N_{nitrate}$ values of around −10‰ to +2‰ (Kendall & McDonnell, 1998; Mayer et al., 2001). The latter process is likely also responsible for the nitrate in spring 27 with −0.6‰ and low NO_3^- concentrations of 0.27 mmol/L.

Therefore, Figure 3 and Table 2 indicate that the isotopic compositions of nitrate in groundwater are consistent with nitrate being derived from manure predominantly in the younger groundwater and mineralization of organic nitrogen in agricultural and forest soil, and potentially nitrification of ammonia and urea containing fertilizers predominantly in the groundwater with higher MTTs.

4.5. Processes Regulating Denitrification in Groundwater

The initial isotopic compositions of nitrate can be further modified by N and O isotope fractionation during processes such as denitrification. During this process, ^{15}N and ^{18}O are progressively enriched in the remaining nitrate as concentrations decrease. In laboratory studies, $\delta^{15}N$:$\delta^{18}O$ trajectories of 1 are observed for denitrification (Wunderlich et al., 2012). However, in freshwater systems empirical $\delta^{15}N$:$\delta^{18}O$ trajectories of 0.5 to 0.8 were detected (Amberger & Schmidt, 1987; Casciotti et al., 2002). Trajectories of <1 in aquifers may be explained by changing redox conditions (oxic/anoxic) leading to a masking of isotopic systematics of denitrification with those of nitrification or by the back reaction of NO_2^- to NO_3^- and anammox (Granger & Wankel, 2016; Wunderlich et al., 2012). In Figure 3 two straight lines with a slope of 0.5 and 0.8 were inserted inversely from the two data points with the most elevated $\delta^{15}N$ and $\delta^{18}O$ in nitrate (GWM 64 and GWM 65 in the perched aquifer). Assuming an initial δ_{R_0} for $\delta^{18}O$ of 1.7‰, we determined the initial δ_{R_0} for $\delta^{15}N$ for GWM 64, GWM 65, the three spring pools and well 50.

$$\frac{\delta_{R_t}}{\delta_{R_0}} = \frac{C_t}{C_0}^{(\alpha-1)} \tag{5}$$

δ_{R_t} is the $\delta^{15}N$ value of the reactant nitrate at time t, δ_{R_0} is the initial $\delta^{15}N$ value of nitrate, C_t and C_0 represent the concentrations of nitrate at times t and zero, respectively, and α is the isotopic fractionation factor

To estimate the extent of biodegradation B along the flow path between two sampling points equation 6 can be used:

$$B[\%] = 1 - \frac{\delta_{R_t}}{\delta_{R_0}}^{\frac{1000}{\epsilon}} \tag{6}$$

B denotes the percentage of nitrate reduced from time zero to t, δ_{R_t} and δ_{R_0} are the $\delta^{15}N$ values of nitrate, and ϵ is the N isotope enrichment factor.

Using equation (6), derived from equation (5) by Rayleigh (1896) & Mariotti et al. (1981), and a characteristic N isotope enrichment factor ϵ of −15.9‰ for porous groundwater systems (Boettcher et al., 1990), we calculated the initial nitrate concentration. The results in Table 3 demonstrate that denitrification removed between 24% and 51% of the initial groundwater nitrate obtained from the two wells (GWMs 64 and 65) displaying denitrification trends. Furthermore, nitrate reduction by denitrification was also assessed for the three spring pools. For spring pool 2 a nitrate reduction of 26% to 39% was calculated and 13% to 28% for spring pools 1 and 3, indicating only little nitrate reduction. Furthermore, one well (well 50) in the main aquifer shows slightly

Table 3

Calculated Results to Interpret the $\delta^{15}N_{nitrate}$ and $\delta^{18}O_{nitrate}$ Values GWM 64 and 65, Spring Pool 1, 2, and 3 in the Perched Aquifer and Well 50 in the Main Aquifer

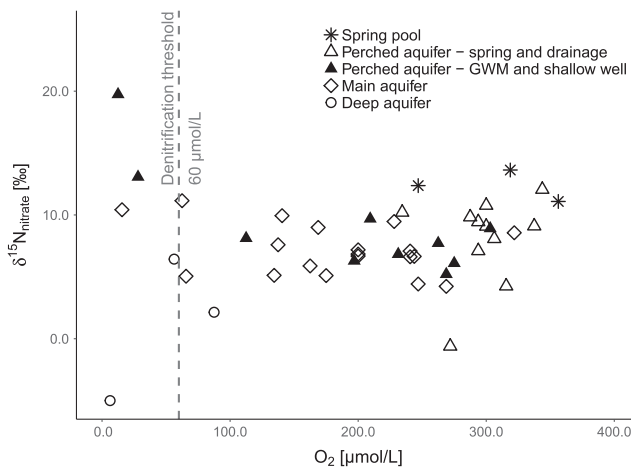|	$C_{t-NO_3^-}$	$\delta^{15}N_t$	$\delta^{18}O_t$	slope	$\delta^{15}N_0$	$\delta^{18}O_0 = 1,7‰$ $C_{0-NO_3^-}$	$\%_{red.}$
	(mmol/L)	(‰)	(‰)	(-)	(‰)	(mmol/L)	(%)
GWM 64	0.32	19.7	7.5	0.5	8.1	0.69	51%
				0.8	12.5	0.52	36%
GWM 65	0.14	13.1	5.2	0.5	6.1	0.22	35%
				0.8	8.7	0.19	24%
Spring pool 1	0.38	13.6	3.5	0.5	10	0.48	20%
				0.8	11.4	0.44	13%
Spring pool 2	0.85	11.1	5.6	0.5	3.3	1.42	39%
				0.8	6.2	1.17	26%
Spring pool 3	0.57	12.4	4.3	0.5	7.2	1.1	28%
				0.8	9.2	0.97	18%
Well 50	0.21	11.2	5.1	0.5	6.6	0.28	25%
				0.8	8.3	0.25	16%

elevated $\delta^{18}O$ values above the shaded area, but nitrate reduction calculated with the Rayleigh equation shows only minor reduction with less than 30% of the initial nitrate concentration reduced.

Only two wells in the perched aquifer (GWMs 64 and 65) produced groundwater with elevated $\delta^{15}N$ values in combination with O_2 concentrations of less than 60 µmol/L and low NO_3^- concentrations potentially indicating some denitrification (Figures 6 and 7). However, Figure 7 shows that $\delta^{15}N$ is not increasing with decreasing NO_3^- concentration and increasing depths within the aquifer and consequently increasing travel time, indicating that there is no general trend for denitrification in the data set of the study area.
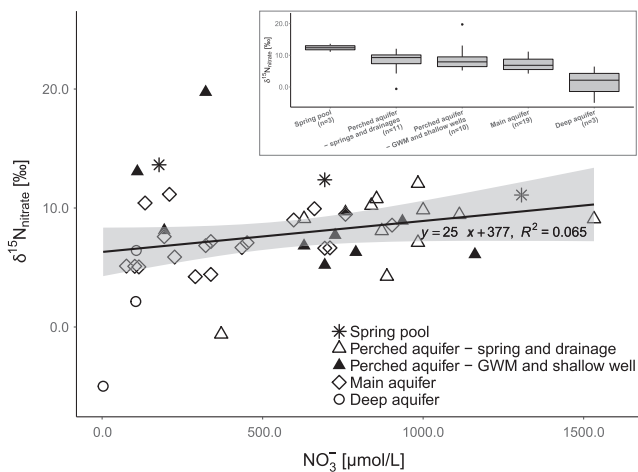
At the two GWM sites, reducing redox conditions with dissolved O_2 concentrations of less than 60 µmol/L were observed (Böhlke et al., 2002; Tesoriero & Puckett, 2011) suggesting that denitrification occurs in this groundwater system at O_2 threshold concentrations of less than 60 µmol/L. Hence, there is some evidence for denitrification if a combination of elevated $\delta^{15}N$ and $\delta^{18}O$ values and O_2 concentrations <60 µmol/L occur, which is the case for only two groundwater samples from GWM 65 and GWM 64 (Figure 6). However, GWM 64 is located in close proximity to an old landfill and is probably influenced by its highly reducing effluent. At GWM 65, there is a thick layer of silty sediments from 1 to 10 mbgl in the well log resulting in a untypical facies distribution for the entire study area that may be the reason for facilitating denitrification at this site.

Figure 6. Plot of $\delta^{15}N_{nitrate}$ against O_2 concentrations to determine potential denitrification; The O_2 threshold concentration of 60 µmol/L has been drawn in with a dashed line.

Analyses of $\delta^{34}S$ in sulfate (Figure 4) indicate pyrite oxidation in the deep aquifer with negative $\delta^{34}S$ values of −8.2‰ from groundwater from well 73 and −2.5‰ from well 59. These observations are also in accordance with Schwientek et al. (2008), who found distinctly negative $\delta^{34}S_{sulfate}$ values of up to −15‰ in the groundwater of the South-German Molasse basin as a result of nitrate dependent pyrite oxidation. However, $\delta^{15}N$ values are low (−5.0‰ and 6.4‰, respectively) and therefore denitrification appears not to be prevalent. In addition, S and O isotope compositions in agricultural fertilizers and S isotope compositions of animal slurries have been reported by Moncaster et al. (2000) and Bartlett et al. (2010) (Figure 4). Since the groundwater sulfate in the wells was characterized by $\delta^{34}S$ values of around 5‰ accompanied with moderate SO_4^{2-} concentrations of 0.2 to 0.4 mmol/L and elevated NO_3^- concentrations between approximately 0.7 and 1 mmol/L, it is suggested that $\delta^{34}S$ values in dissolved SO_4^{2-} are predominantly affected by animal slurry or chemical S fertilizer-derived S (Einsiedl, 2012). Hence, the presented results show that denitrification may occur only in two exceptional cases in the aquifers of the study area. The

Figure 7. Plot of $\delta^{15}N_{nitrate}$ against NO_3^- concentrations to determine the denitrification potential, shaded area displays 95% confidence interval of data points; boxplot in the right corner shows $\delta^{15}N_{nitrate}$ distribution over the aquifer units.

lack of denitrification appears to be caused by high O_2 concentrations in the groundwater. Therefore, we further explored the relation of O_2 reduction rates, denitrification lag times, and denitrification potential.

4.6. Denitrification Lag Times and O_2 Reduction Rates

The O_2 concentration is a crucial parameter for preventing the occurrence of denitrification. In other field studies, a strong correlation of O_2 concentrations and denitrification potential was observed as there was only denitrification detected, when O_2 concentrations were less than 60 µmol/L (Böhlke et al., 2002; Tesoriero & Puckett, 2011). These results are consistent with our findings that denitrification does not occur when O_2 concentrations are above 60 µmol/L, which is the case in all, but two groundwater samples.

4.6.1. Zeroth-Order Versus First-Order O_2 Reduction Rates

To determine the lag phase for denitrification, which is the time needed to lower the O_2 concentration below the denitrification threshold of 60 µmol/L, we calculated the O_2 reduction rate for the aquifer and estimated the availability of electron donors for nitrate reduction using zeroth-order (rate independent of concentration) and first-order kinetics (rate dependent of concentration; Appelo & Postma, 2005; Böhlke et al., 2002). In Figure 5, the O_2 concentrations of groundwater from the perched aquifer and main aquifer are plotted against the apparent MTTs modeled with a dispersion model. As there were only few wells available in the main aquifer for which the apparent groundwater MTT could be modeled with a simple dispersion model, where no mixing of old ^{3}H-free anoxic and young groundwater occurred, the data points with apparent MTT > 25 years are relatively sparse but reveal, nevertheless, a well-defined regression line for zeroth- and first-order kinetics ($R_0^2 = 0.77$, $R_1^2 = 0.84$). First-order kinetics show a somewhat better fit ($R_1^2 = 0.84$) and are therefore the preferred model. However, first-order kinetics are only valid when the substrate concentration S is lower than the half-saturation constant K_s, whereas zeroth-order kinetics are only valid at high-substrate concentrations (Bekins et al., 1998; Rifai & Bedient, 1990). This was not tested for the studied aquifer, and consequently, both zeroth-order and first-order models are shown in Figure 5. We advise that future studies should determine K_s, v_{max} (maximal removal time), Y (yield), and the parameter b (microbial decay rate) to determine the degradation and the microbial growth rate over all concentration ranges of the substrate pool in laboratory studies. According to Figure 5, the O_2 reduction rate is 2.2 µmol/(L·year) for the zeroth-order kinetics and 0.015 1/year for the first-order kinetics, which is relatively low compared to DOC-rich waters in shallow riparian flow paths that have O_2 reduction rates of up to 140 µmol/(L·year) for zerorh-order kinetics (Tesoriero & Puckett, 2011). Assuming that the input is air-saturated groundwater with an O_2 concentration of ~330 µmol/L (Appelo & Postma, 2005), it takes around 114 years assuming first-order kinetics until the O_2 concentration has been reduced to less than 60 µmol/L in order to obtain redox conditions favorable for denitrification. In the literature, denitrification lag times vary widely between different study sites, ranging from <20 years at sites with high O_2 reduction rates and a high availability of electron donors to >60 years at sites with low O_2 reduction rates and a very limited supply of electron donors (Tesoriero & Puckett, 2011). Our findings of a denitrification lag time of >100 years are on the very high end of the previously reported range.

4.6.2. Implications of O_2 Reduction Rates in Porous Aquifers

We propose that the calculation of O_2 reduction rates in groundwater is of critical importance for estimating the time required until denitrification may commence in an aquifer and thereby accelerating nitrate removal. This approach may improve the assessment of the vulnerability of aquifers posed by dissolved nitrate and its persistence in drinking water resources. Fogg et al. (1984) have previously concluded that nitrate-vulnerable areas may be best identified in combination with the assessment of MTTs. To further include areas with low nitrate reduction via denitrification, we propose that the assessment of O_2 reduction rates for potential nitrate reduction is a powerful tool to determine the potential of suboxic redox processes such as denitrification to occur and should be considered in future groundwater vulnerability studies. If the O_2 reduction is low in a groundwater system and there is no major change in the availability of reactive donors with increasing aquifer depth, denitrification will still not occur over extended time periods, also if O_2 concentrations fall below threshold values, where denitrification can occur. Consequently, elevated concentrations of nitrate will persist at time scales equal to the estimated apparent MTT of groundwater at drinking water wells. An intensive agriculturally used ecosystem with no or only little nitrate reduction potential may therefore be

of great risk for exceeding drinking water quality guidelines for many years or decades after contamination has occurred. Moreover, elevated nitrate concentrations in groundwater would be a concern for surface water quality (Carpenter et al., 1998), if a hydraulic connection between groundwater and the rivers Isar and Danube is present.

The obtained results illustrate the importance of the determination of apparent MTTs of groundwater linked with the calculation of O_2 reduction rates to predict the rate at which nitrate may be removed from groundwater through the process of denitrification. This approach increases the understanding of the groundwater ecosystem and facilitates the assessment of the vulnerability of aquifers posed by dissolved nitrate and its persistence in drinking water resources.

5. Conclusion

The calculated O_2 reduction rate of 0.015 1/year for first-order kinetics is relatively low in the studied aquifer and leads to a high denitrification lag phase of approximately 114 years. In consequence, we suggest that the lack of microbial available electron donors in the aquifer is responsible for the low O_2 reduction rates and the high nitrate concentrations in this groundwater system. We therefore demonstrate that this approach is highly effective in estimating the approximate residence time of nitrate and the assessment of nitrogen loads in groundwater. Hence, the results provide critical information on the vulnerability of aquifers posed by dissolved nitrate and the time frames required to achieve water quality improvements in nitrate-polluted aquifers.

For groundwater ecosystems with a low potential for the reduction of redox sensitive parameters such as nitrate, we recommend a reduction of anthropogenic N inputs by applying agricultural beneficial management practices (Asgedom & Kebreab, 2011). In situ groundwater remediation has also been shown to be suitable and effective to remove nitrate and consequently reach acceptable drinking water quality; however, this approach may be challenging in such heterogeneous groundwater systems and potentially too costly (Archna & Sobti, 2012; Della Rocca et al., 2007; Janda et al., 1988).

Acronyms

BMM	Binary mixing model
DOC	Dissolved organic carbon
EC	Electrical conductivity
GWM	Groundwater monitoring station
MTT	Mean transit time
TOC	Total organic carbon

References

Amberger, A., & Schmidt, H. L. (1987). Natürliche Isotopengehalte von Nitrat als Indikatoren für dessen Herkunft. *Geochimica et Cosmochimica Acta*, *51*(10), 2699–2705. https://doi.org/10.1016/0016-7037(87)90150-5

Appelo, C. A. J., & Postma, D. (2005). *Geochemistry, groundwater and pollution* (2nd ed.), 647 pp. London, New York: A.A. Balkema Publishers, Taylor & Francis Group plc.

Aravena, R., Evans, M. L., & Cherry, J. A. (1993). Stable isotopes of oxygen and nitrogen in source identification of nitrate from septic systems. *Ground Water*, *31*(2), 7.

Aravena, R., & Wassenaar, L. I. (1993). Dissolved organic carbon and methane in a regional confined aquifer, southern Ontario, Canada: Carbon isotope evidence for associated subsurface sources. *Applied Geochemistry*, *8*(5), 483–493. https://doi.org/10.1016/0883-2927(93)90077-T

Archna, S. K. S., & Sobti, R. C. (2012). Nitrate removal from ground water: A review. *E-Journal of Chemistry*, *9*(4), 1667–1675. https://doi.org/10.1016/S0043-1354(87)80018-0

Asgedom, H., & Kebreab, E. (2011). Beneficial management practices and mitigation of greenhouse gas emissions in the agriculture of the Canadian Prairie: A review. *Agronomy for Sustainable Development*, *31*(3), 433–451. https://doi.org/10.1007/s13593-011-0016-2

Bartlett, R., Bottrell, S. H., Sinclair, K., Thornton, S., Fielding, I. D., & Hatfield, D. (2010). Lithological controls on biological activity and groundwater chemistry in Quaternary sediments. *Hydrological Processes*, *24*(6), 726–735. https://doi.org/10.1002/hyp.7514

Bekins, B. A., Warren, E., & Godsy, E. M. (1998). A comparison of zero-order, first-order and Monod biotransformations models. *Groundwater*, *36*(2), 261–268.

Boettcher, J., Strebel, O., Voerkelius, S., & Schmidt, H. L. (1990). Using isotope fractionation of nitrate-nitrogen and nitrate-oxygen for evaluation of microbial denitrification in a sandy aquifer. *Journal of Hydrology*, *114*(3-4), 413–424. https://doi.org/10.1016/0022-1694(90)90068-9

Böhlke, J. K. (2002). Groundwater recharge and agricultural contamination. *Hydrogeology Journal*, *10*(1), 153–179. https://doi.org/10.1007/s10040-001-0183-3

Böhlke, J. K., & Denver, J. M. (1995). Combined use of groundwater dating, chemical, and isotopic analyses to resolve the history and fate of nitrate contamination in two agricultural watersheds, atlantic coastal Plain, Maryland. *Water Resources Research*, *31*(9), 2319–2339. https://doi.org/10.1029/95WR01584

Böhlke, J., Ericksen, G., & Revesz, K. (1997). Stable isotope evidence for an atmospheric origin of desert nitrate deposits in northern Chile and southern California, U.S.A. *Chemical Geology*, *136*(1-2), 135–152. https://doi.org/10.1016/S0009-2541(96)00124-6

Böhlke, J. K., Wanty, R., Tuttle, M., Delin, G., & Landon, M. (2002). Denitrification in the recharge area and discharge area of a transient agricultural nitrate plume in a glacial outwash sand aquifer, Minnesota. *Water Resources Research*, *38*(7), W1105. https://doi.org/10.1029/2001WR000663

Bonin, P., Gilewicz, M., & Bertrand, J. C. (1989). Effects of oxygen on each step of denitrification on Pseudomonas nautica. *Canadian Journal of Microbiology*, *35*(11), 1061–1064. https://doi.org/10.1139/m89-177

Buchwald, C., Santoro, A. E., McIlvin, M. R., & Casciotti, K. L. (2012). Oxygen isotopic composition of nitrate and nitrite produced by nitrifying cocultures and natural marine assemblages. *Limnology and Oceanography*, *57*(5), 1361–1375. https://doi.org/10.4319/lo.2012.57.5.1361

Calderer, M., Gibert, O., Martí, V., Rovira, M., De Pablo, J., Jordana, S., et al. (2010). Denitrification in presence of acetate and glucose for bioremediation of nitrate-contaminated groundwater. *Environmental Technology*, *31*(7), 799–814. https://doi.org/10.1080/09593331003667741

Carpenter, S. R., Caraco, N. F., Correll, D. L., Howarth, R. W., Sharpley, A. N., & Smith, V. H. (1998). Nonpoint pollution of surface waters with phosphorus and nitrogen. *Ecological Applications*, *8*(1998), 559–568. https://doi.org/10.1890/1051-0761(1998)008[0559:NPOSWW]2.0.CO;2

Casciotti, K. L., McIlvin, M., & Buchwald, C. (2010). Oxygen isotopic exchange and fractionation during bacterial nitrite oxidation. *Limnology and Oceanography*, *55*(3), 1064–1074.

Casciotti, K. L., Sigman, D. M., Hastings, M. G., Bohlke, J. K., & Hilkert, A. (2002). Measurement of the oxygen isotopic composition of nitrate seawater and freshwater using the denitrifier method. *Analytical Chemistry*, *74*(19), 4905–4912. https://doi.org/10.1021/ac020113w

Choi, W. J., Han, G. H., Lee, S. M., Lee, G. T., Yoon, K. S., Choi, S. M., & Ro, H. M. (2007). Impact of land-use types on nitrate concentration and δ^{15}N in unconfined groundwater in rural areas of Korea. *Agriculture, Ecosystems and Environment*, *120*(2-4), 259–268. https://doi.org/10.1016/j.agee.2006.10.002

Clark, I. (2015). *Groundwater geochemistry and isotopes* (647 pp.). Boca Raton, FL: CRC Press.

Clark, I. D., & Fritz, P. (1997). *Environmental isotopes in hydrogeology* (344 pp.). Boca Raton, FL: CRC Press.

Davies, K. J. P., Lloyd, D., & Boddy, L. (1989). The effect of oxygen on denitrification in Paracoccus denitrificans and Pseudomonas aeruginosa. *Microbiology*, *135*(9), 2445–2451. https://doi.org/10.1099/00221287-135-9-2445

Della Rocca, C., Belgiorno, V., & Meriç, S. (2007). Overview of in-situ applicable nitrate removal processes. *Desalination*, *204*(1-3 SPEC. ISS.), 46–62. https://doi.org/10.1016/j.desal.2006.04.023

Doppler, G., Heissig, K., & Reichenbacher, B. (2005). Die Gliederung des Tertiaers im sueddeutschen Molassebecken. *Newsletters on Stratigraphy*, *41*(1), 359–375. https://doi.org/10.1127/0078-0421/2005/0041-0359

Durka, W., Schulze, E.-D., Gebauer, G., & Voerkellus, S. (1994). Effects of forest decline on uptake and leaching of deposited nitrate determined from ^{15}N and ^{18}O measurements. *Nature*, *372*(22/29), 765–767.

Einsiedl, F. (2012). Sea-water/groundwater interactions along a small catchment of the European Atlantic coast. *Applied Geochemistry*, *27*(1), 73–80. https://doi.org/10.1016/J.APGEOCHEM.2011.09.004

Einsiedl, F., Hertkorn, N., Wolf, M., Frommberger, M., Schmitt-Kopplin, P., & Koch, B. P. (2007). Rapid biotic molecular transformation of fulvic acids in a karst aquifer. *Geochimica et Cosmochimica Acta*, *71*(22), 5474–5482. https://doi.org/10.1016/j.gca.2007.09.024

Einsiedl, F., Maloszewski, P., & Stichler, W. (2009). Multiple isotope approach to the determination of the natural attenuation potential of a high-alpine karst system. *Journal of Hydrology*, *365*(1-2), 113–121. https://doi.org/10.1016/j.jhydrol.2008.11.042

Einsiedl, F., & Mayer, B. (2006). Hydrodynamic and microbial processes controlling nitrate in a fissured-porous karst aquifer of the Franconian Alb, southern Germany. *Environmental Science & Technology*, *40*(21), 6697–702. https://doi.org/10.1021/es061129x

European Commision (2012). Commission staff working document, European overview (2/2) accompanying the document: Report from the commission to the European Parliament and the council on the implementation of the water framework directive (2000/60/EC) river basin management plans (Tech. Rep) Brussels: European Commision.

European Commision (2015). The water framework directive and the floods directive: Actions towards the good status of EU water and to reduce flood risks (Tech. Rep) Brussels: European Commisson.

European Community (2000). Directive 2000/60/EC of the European Parliament and of the Council of 23 October 2000 establishing a framework for community action in the field of water policy. *Official Journal of the European Parliament*, *L327*(September 1996), 1–82. https://doi.org/10.1039/ap9842100196

Fang, Y., Koba, K., Makabe, A., Zhu, F., Fan, S., Liu, X., & Yoh, M. (2012). Low δ18O values of nitrate produced from nitrification in temperate forest soils. *Environmental Science and Technology*, *46*(16), 8723–8730. https://doi.org/10.1021/es300510r

Fogg, G. E., LaBolle, E. M., & Weissmann, G. S. (1999). Groundwater vulnerability assessment: Hydrologic perspective and example from Salinas Valley, California. In *Assessment of non-point source pollution in the Vadose Zone, Geophysical Monograph Series* (pp. 45–61). Washington, DC: American Geophysical Union.

Grabczak, J., Rozanski, K., Maloszewski, P., & Zuber, A. (1984). Estimation of the tritium input function with the aid of stable isotopes. *Catena*, *11*(2-3), 105–114. https://doi.org/10.1016/0341-8162(84)90001-8

Granger, J., & Wankel, S. D. (2016). Isotopic overprinting of nitrification on denitrification as a ubiquitous and unifying feature of environmental nitrogen cycling. *Proceedings of the National Academy of Sciences*, *113*(42), E6391—E6400. https://doi.org/10.1073/pnas.1601383113

Hamdi, W., Gamaoun, F., Pelster, D. E., & Seffen, M. (2013). Nitrate sorption in an agricultural soil profile. *Applied and Environmental Soil Science*, *2013*(3), 7. https://doi.org/10.1155/2013/597824

Hansen, B., Thorling, L., Dalgaard, T., & Erlandsen, M. (2011). Trend reversal of nitrate in Danish groundwater—A reflection of agricultural practices and nitrogen surpluses since 1950. *Environmental Science & Technology*, *45*(1), 228–234. https://doi.org/10.1021/es102334u

Harper, B. H. J. (1924). The accurate determination of nitrates in soils—Phenoldisulfonic acid method. *Industrial and Engineering Chemistry*, *16*(2), 180–183.

Hochstein, L. I., Betlach, M., & Kritikos, G. (1984). The effect of oxygen on denitrification during steady-state growth of Paracoccus halodenitrificans. *Archives of Microbiology*, *137*(1), 74–78. https://doi.org/10.1007/bf00425811

Hollocher, T. C. (1984). Source of the oxygen atoms of nitrate in the oxidation of nitrite by Nitrobacter agilis and evidence against a PON anhydride mechanism in oxidative phosphorylation. *Archives of Biochemistry and Biophysics*, *233*(2), 721–727. https://doi.org/10.1016/0003-9861(84)90499-5

Hooda, P., Edwards, A., Anderson, H., & Miller, A. (2000). A review of water quality concerns in livestock farming areas. *Science of The Total Environment*, *250*(1-3), 143–167. https://doi.org/10.1016/S0048-9697(00)00373-9

Janda, V., Rudovský, J., Wanner, J., & Marha, K. (1988). In situ denitrification of drinking water. *Water Science and Technology*, *20*(3), 215–219. https://doi.org/10.2166/wst.1988.0101

Jurgens, B. C., Böhlke, J. K., & Eberts, S. M. (2012). TracerLPM (Version 1): An Excel workbook for interpreting groundwater age distributions from environmental tracer data (Tech. Rep. Version 1). Reston, VA: U.S. Department of the Interior, U.S Geological Survey.

Kainzmaier, B., Thom, P., Wrobel, M., & Pukowietz, C. (2007). *Geowissenschaftliche Landesaufnahme in der Planungsregion 13 Landshut: Erläuterungen zur Hydrogeologischen Karte* (232 pp.). Augsburg, Germany: Bayrisches Landesamt für Umwelt.

Katz, B. G., Chelette, A. R., & Pratt, T. R. (2004). Use of chemical and isotopic tracers to assess nitrate contamination and ground-water age, Woodville Karst Plain, USA. *Journal of Hydrology*, *289*(1-4), 36–61. https://doi.org/10.1016/j.jhydrol.2003.11.001

Kendall, C., & McDonnell, J. J. (1998). *Isotope tracers in catchment hydrology* (839 pp.). Amsterdam: Elsevier Ltd. https://doi.org/10.1016/B978-0-444-81546-0.50024-0

Knöller, K., Vogt, C., Haupt, M., Feisthauer, S., & Richnow, H. H. (2011). Experimental investigation of nitrogen and oxygen isotope fractionation in nitrate and nitrite during denitrification. *Biogeochemistry*, *103*(1), 371–384. https://doi.org/10.1007/s10533-010-9483-9

Koh, D. C., Mayer, B., Lee, K. S., & Ko, K. S. (2010). Land-use controls on sources and fate of nitrate in shallow groundwater of an agricultural area revealed by multiple environmental tracers. *Journal of Contaminant Hydrology*, *118*(1-2), 62–78. https://doi.org/10.1016/j.jconhyd.2010.08.003

Körner, H., & Zumft, W. G. (1989). Expression of denitrification enzymes in response to the dissolved oxygen level and respiratory substrate in continuous culture of Pseudomonas stutzeri. *Applied and Environmental Microbiology*, *55*(7), 1670–1676.

Kreft, A., & Zuber, A. (1978). On the physical meaning of the dispersion equation and its solutions for different initial and boundary conditions. *Chemical Enigneering Science*, *33*, 1471–1480.

Kroopnick, P., & Craig, H. (1972). Atmospheric oxygen: Isotopic composition and solubility fractionation. *Science*, *175*(4017), 54–55. https://doi.org/10.1126/science.175.4017.54

Lill, T. (2013). Schweinemast: Bayern wird zum riesigen Saustall.

Maloszewski, P. M. A., Rauert, W., Stichler, W., & Herrmann, A. (1983). Application of flow models in an alpine catchment area using tritium and deuterium. *Journal of Hydrology*, *66*, 319–330.

Maloszewski, P., Stichler, W., Zuber, A., & Rank, D. (2002). Identifying the flow systems in a karstic-fissured-porous aquifer, the Schneealpe, Austria, by modelling of environmental ^{18}O and ^{3}H isotopes. *Journal of Hydrology*, *256*(1-2), 48–59. https://doi.org/10.1016/S0022-1694(01)00526-1

Maloszewski, P., & Zuber, A. (1982). Determining the turnover time of groundwater systems with the aid of environmental tracers. *Journal of Hydrology*, *57*(3-4), 207–231. https://doi.org/10.1016/0022-1694(82)90147-0

Małoszewski, P., & Zuber, A. (1985). On the theory of tracer experiments in fissured rocks with a porous matrix. *Journal of Hydrology*, *79*(3-4), 333–358. https://doi.org/10.1016/0022-1694(85)90064-2

Maloszewski, P., & Zuber, A. (1996). Lumped parameter models for the interpretation of environmental tracer data. *Manual on Mathematical Models in Isotope Hydrogeology*, *IAEA-TECDO*, 9–58.

Mariotti, A., Germon, J. C., Hubert, P., Kaiser, P., Letolle, R., & Tardieux, P. (1981). Experimental determination of nitrogen kinetic isotope fractionation: Some principles; illustration for the denitrification and nitrification processes. *Plant Soil*, *62*(7), 413–430. https://doi.org/10.1007/BF02374138

Mariotti, A., Landreau, A., & Simon, B. (1988). ^{15}N isotope biogeochemistry and natural denitrification process in groundwater: Application to the chalk aquifer of northern France. *Geochimica et Cosmochimica Acta*, *52*(7), 1869–1878. https://doi.org/10.1016/0016-7037(88)90010-5

Massmann, G., Sültenfuß, J., Dünnbier, U., Knappe, A., Taute, T., & Pekdeger, A. (2007). Investigation of groundwater residence times during bank filtration in Berlin: A multi-tracer approach. *Hydrological Processes*, *22*(November 2008), 788–801. https://doi.org/10.1002/hyp.6649

Mayer, B., Bollwerk, S. M., Mansfeldt, T., Hütter, B., & Veizer, J. (2001). The oxygen isotope composition of nitrate generated by nitrification in acid forest floors. *Geochimica et Cosmochimica Acta*, *65*(16), 2743–2756. https://doi.org/10.1016/S0016-7037(01)00612-3

Mayer, B., Boyer, E. W., Goodale, C., Jaworski, N. A., van Breemen, N., Howarth, R. W., et al. (2002). Sources of nitrate in rivers draining sixteen watersheds in the northeastern U.S.: Isotopic constraints. *Biogeochemistry*, *57*(1), 171–197. https://doi.org/10.1023/A:1015744002496

Moncaster, S. J., Bottrell, S. H., Tellam, J. H., Lloyd, J. W., & Konhauser, K. O. (2000). Migration and attenuation of agrochemical pollutants: Insights from isotopic analysis of groundwater sulphate. *Jounral of Contaminant Hydrology*, *43*(2), 147–163. https://doi.org/10.1016/S0169-7722(99)00104-7

Payne, W. J. (1983). Bacterial denitrification: Asset or defect? *BioScience*, *33*(5), 319–325.

Piotrowska, N. (2013). Status report of AMS sample preparation laboratory at GADAM Centre, Gliwice, Poland. *Nuclear Instruments and Methods in Physics Research B*, *294*, 176–181. https://doi.org/10.1016/j.nimb.2012.05.017

Rayleigh, J. W. S. (1896). Theoretical considerations respecting the separation of gases by diffusion and similar processes. *Philosophical Magazine*, *42*, 493–498.

Rifai, H. S., & Bedient, P. B. (1990). Comparison of biodegradation kinetics with an instantaneous reaction model for groundwater. *Water Resources Research*, *26*(4), 637–645. https://doi.org/10.1029/WR026i004p00637

Rivett, M. O., Buss, S. R., Morgan, P., Smith, J. W., & Bemment, C. D. (2008). Nitrate attenuation in groundwater: A review of biogeochemical controlling processes. *Water Research*, *42*(16), 4215–4232. https://doi.org/10.1016/j.watres.2008.07.020

Robertson, L. A., & Kuenen, J. G. (1984). Aerobic denitrification: A controversy revived. *Archives of Microbiology*, *139*(4), 351–354. https://doi.org/10.1007/BF00408378

Schwientek, M., Einsiedl, F., Stichler, W., Stögbauer, A., Strauss, H., & Maloszewski, P. (2008). Evidence for denitrification regulated by pyrite oxidation in a heterogeneous porous groundwater system. *Chemical Geology*, *255*(1-2), 60–67. https://doi.org/10.1016/j.chemgeo.2008.06.005

Sebilo, M., Billen, G., Mayer, B., Billiou, D., Grably, M., Garnier, J., & Mariotti, A. (2006). Assessing nitrification and denitrification in the Seine River and estuary using chemical and isotopic techniques. *Ecosystems*, *9*(4), 564–577. https://doi.org/10.1007/s10021-006-0151-9

Sebilo, M., Mayer, B., Nicolardot, B., Pinay, G., & Mariotti, A. (2013). Long-term fate of nitrate fertilizer in agricultural soils. *Proceedings of the National Academy of Sciences*, *110*(45), 18,185–18,189. https://doi.org/10.1073/pnas.1305372110

Silva, S., Kendall, C., Wilkison, D., Ziegler, A., Chang, C., & Avanzino, R. (2000). A new method for collection of nitrate from fresh water and the analysis of nitrogen and oxygen isotope ratios. *Journal of Hydrology*, *228*(1-2), 22–36. https://doi.org/10.1016/S0022-1694(99)00205-X

Singh, B. R., & Kanehiro, Y. (1969). Adsorption of nitrate in amorphous and kaolinitic Hawaiian soils. *Soil Science Society of America Journal*, *33*, 681–683.

Smith, R. L., Kent, D. B., Repert, D. A., & Böhlke, J. (2016). Anoxic nitrate reduction coupled with iron oxidation and attenuation of dissolved arsenic and phosphate in a sand and gravel aquifer. *Geochimica et Cosmochimica Acta*, *196*, 102–120. https://doi.org/10.1016/j.gca.2016.09.025

Snider, D. M., Spoelstra, J., Schiff, S. L., & Venkiteswaran, J. J. (2010). Stable oxygen isotope ratios of nitrate produced from nitrification: ^{18}O-labeled water incubations of agricultural and temperate forest soils. *Environmental Science & Technology*, *44*(14), 5358–5364. https://doi.org/10.1021/es1002567

Starr, R. C., & Gillham, R. W. (1993). Denitrification and organic carbon availability in two aquifers. *Ground Water*, *31*(6), 934–947. https://doi.org/10.1111/j.1745-6584.1993.tb00867.x

Stichler, W., & Herrmann, A. (1983). Application of environmental isotope techniques in water balance studies of small basins. *New Approaches in Water Balance Computations*, *18*(148), 93–112.

Stoewer, M., Knöller, K., & Stumpp, C. (2015). Tracing freshwater nitrate sources in pre-alpine groundwater catchments using environmental tracers. *Journal of Hydrology*, *524*, 753–767. https://doi.org/10.1016/j.jhydrol.2015.03.022

Stumpp, C., Klaus, J., & Stichler, W. (2014). Analysis of long-term stable isotopic composition in german precipitation. *Journal of Hydrology*, *517*, 351–361. https://doi.org/10.1016/j.jhydrol.2014.05.034

Suchy, M., Wassenaar, L. I., Graham, G., & Zebarth, B. (2018). High-frequency NO_3- isotope ($\delta^{15}N$, $\delta^{18}O$) patterns in ground water recharge reveal that short-term land use and climatic changes influence nitrate contamination trends. *Hydrology and Earth System Sciences Discussion*, *22*(February), 1–27. https://doi.org/10.5194/hess-2018-35

Sültenfuß, J. (1998). The radionuclide Tritium in the ocean: Measurement and distribution of Tritium in the South Atlantic and Weddell Sea (PhD thesis), Bremen University.

Sültenfuß, J., & Massmann, G. (2004). Datierung mit der ^{3}He-Tritium-Methode am Beispiel der Uferfiltration im Oderbruch. *Grundwasser*, *9*(4), 221–234. https://doi.org/10.1007/s00767-004-0055-6

Sültenfuß, J., Roether, W., & Rhein, M. (2009). The Bremen mass spectrometric facility for the measurement of helium isotopes, neon, and tritium in water. *Isotopes in Environmental and Health Studies*, *45*(2), 83–95. https://doi.org/10.1080/10256010902871929

Taylor, P. G., & Townsend, A. R. (2010). Stoichiometric control of organic carbon-nitrate relationships from soils to the sea. *Nature*, *464*(7292), 1178–1181. https://doi.org/10.1038/nature08985

Tesoriero, A. J., Liebscher, H., & Cox, S. E. (2000). Mechanism and rate of denitrification in an agricultural watershed: Electron and mass balance along groundwater flow paths. *Water Resources Research*, *36*(6), 1545–1559. https://doi.org/10.1029/2000WR900035

Tesoriero, A. J., & Puckett, L. J. (2011). O_2 reduction and denitrification rates in shallow aquifers. *Water Resources Research*, *47*, W12522. https://doi.org/10.1029/2011WR010471

The Council of the EU (1998). Council directive 98/83/EC of 3 November 1998 on the quality of water intended for human consumption. *Official Journal of the European Communities*, *L330*, 32–54. https://doi.org/2004R0726 - v.7 of 05.06.2013

Tiedje, J. (1988). Ecology of denitrification and dissimilatory nitrate reduction to ammonium. In *Environmental Microbiology on Anaerobes* (pp. 179–244).

Visser, A., Broers, H. P., Purtschert, R., Sültenfuß, J., & De Jonge, M. (2013). Groundwater age distributions at a public drinking water supply well field derived from multiple age tracers (^{85}Kr, $^3H/^3H$, and ^{39}Ar). *Water Resources Research*, *49*, 7778–7796. https://doi.org/10.1002/2013WR014012

Voerkelius, S. (1990). Isotopendiskriminierungen bei der Nitrifikation und Denitrifikation: Grundlagen und Anwendungen der Herkunfts-Zuordnung von Nitrat und Distickstoffmonoxid (PhD thesis), TU, München.

Vogel, J. C., Talma, A. S., & Heaton, T. H. E. (1981). Gaseous nitrogen as evidence for denitrification in groundwater. *Journal of Hydrology*, *50*, 191–200.

Voulvoulis, N., Arpon, K. D., & Giakoumis, T. (2017). The EU water framework directive: From great expectations to problems with implementation. *Science of the Total Environment*, *575*, 358–366. https://doi.org/10.1016/j.scitotenv.2016.09.228

Wassenaar, L. I. (1995). Evaluation of the origin and fate of nitrate in the Abbbotsford aquifer using isotopes of ^{15}N and ^{18}O in NO_3^-. *Applied Geochemistry*, *1995*(10), 391–405. https://doi.org/10.1016/0883-2927(95)00013-A

Wassenaar, L. I., Hendry, M. J., & Harrington, N. (2006). Decadal geochemical and isotopic trends for nitrate in a transboundary aquifer and implications for agricultural beneficial management practices. *Environmental Science & Technology*, *40*(15), 4626–4632. https://doi.org/10.1021/es060724w

Werner, B., & O'Doherty, J. J. (2012). *European waters — Current status and future challenges* (Vol. 9, 53 pp.). Copenhagen: EEA.

Wunderlich, A., Meckenstock, R., & Einsiedl, F. (2012). Effect of different carbon substrates on nitrate stable isotope fractionation during microbial denitrification. *Environmental Science & Technology*, *46*(9), 4861–4868. https://doi.org/10.1021/es204075b